

A Scaling Behavior of Spectral Weight Changes in Perovskite Manganites

$\text{La}_{0.7-y}\text{Pr}_y\text{Ca}_{0.3}\text{MnO}_3$

K. H. Kim¹, J. H. Jung¹, D. J. Eom¹, T. W. Noh^{1,*}, Jaejun Yu², and E. J. Choi³

¹*Department of Physics, Seoul National University, Seoul 151-742, Korea*

²*Department of Physics, Sogang University, Seoul 121-742, Korea*

³*Department of Physics, Seoul City University, Seoul 130-743, Korea*

(February 1, 2008)

Optical conductivity spectra of $\text{La}_{0.7-y}\text{Pr}_y\text{Ca}_{0.3}\text{MnO}_3$ were systematically investigated. For metallic samples, the spectral weight below 0.5 eV, whose magnitude can be represented by the effective carrier number $N_{\text{eff}}(0.5 \text{ eV})$, increases as temperature becomes lower. Regardless of the Pr doping, all the measured values of $N_{\text{eff}}(0.5 \text{ eV})/T_C$ fall into one scaling curve. This scaling behavior could be explained by the theoretical model by Röder *et al.* (Phys. Rev. Lett. **76**, 1356 (1996)), which includes spin double exchange and Jahn-Teller lattice coupling to holes. With the Pr doping, far-infrared conductivities were found to be suppressed, probably due to the Anderson localization.

PACS number; 72.15.Gd, 75.50.Cc, 75.30.Kz, 78.20.Ci

Physics of doped manganites, $R_{1-x}A_x\text{MnO}_3$ (R =rare earth and A =alkaline earth ions) with $0.2 \leq x \leq 0.5$, has been investigated extensively since the recent discovery of colossal magnetoresistance (CMR) phenomena in these compounds. Even if the double exchange (DE) interaction can qualitatively explain most of their physical properties [1], a lot of recent works have revealed that some additional degrees of freedom should be included to describe them more accurately [2–11]. Optical techniques have been useful to address such additional degrees of freedom [2,3,8–10].

However, there still remain some controversies on how to explain temperature(T)-dependent spectral weight (SW) changes in optical spectra of the doped manganites. Especially, there have been numerous interpretations on the mid-infrared (IR) absorption peak below 0.5 eV, which appears below the Curie temperature T_C and becomes stronger at lower temperatures. Okimoto *et al.* claimed that the SW changes should be understood in the spin-split band picture, and they assigned the mid-IR feature to an intraband excitation within an e_g band which was merged below T_C from two spin-split bands [2,3]. Other workers suggested that an orbital degree of freedom should be included to explain the SW changes [4,5], and de Brito and Shiba attributed the mid-IR absorption to an interband transition between the e_g orbital states [5]. Millis *et al.* showed that the dynamic Jahn-Teller (JT) interaction could play an important role in the SW changes [6,7], and Kaplan *et al.* assigned the mid-IR feature to a JT type small polaron absorption [8]. Recently, through detailed studies on optical properties of $\text{La}_{0.7}\text{Ca}_{0.3}\text{MnO}_3$ (LCMO), we proposed that the evolution of the low frequency feature below 0.5 eV come from a crossover from small to large polaron states [10]. In other words, the mid-IR feature should be attributed to an incoherent absorption of a large polaron state, whose existence was predicted by Röder *et al.* [11].

To get further insights on this interesting issue, we investigated optical properties of $\text{La}_{0.7-y}\text{Pr}_y\text{Ca}_{0.3}\text{MnO}_3$ (LPCMO). Hwang *et al.* showed that dc transport properties of LPCMO were affected by a carrier hopping parameter which could be varied systematically by the Pr doping [12]. In this paper, we report on optical conductivity spectra of the LPCMO samples with $y=0.13, 0.4, 0.5$, and 0.7 . We found that detailed conductivity spectra vary significantly with the Pr doping. However, the T -dependence of the SW below 0.5 eV remains similar. Actually, when all of the T -dependent SW are scaled by corresponding T_C values, they fall into one scaling curve. This scaling behavior will be explained using the theoretical results by Röder *et al.* [11].

Polycrystalline LPCMO samples were prepared by a standard solid-state reaction method. The samples were oxygen-annealed at 1100 °C for 72 hours [13]. X-ray diffraction and electron-probe microanalysis measurements confirmed that the samples were single-phase and stoichiometric. Both resistivity and magnetization curves showed hysteretic behaviors, confirming that corresponding phase transitions are of first-order nature [12]. For the samples with $y=0.13, 0.4$, and 0.5 , the metal-insulator (M-I) transition temperatures, defined by temperatures of resistivity maxima in warming (cooling) runs, were 241 (239), 156 (152), and 123 K (118 K), respectively. The $y=0.7$ sample did not show any M-I transition. Values of T_C were estimated from field-cooled dc magnetization curves, which were measured at 100 Oe using a commercial SQUID magnetometer. Due to the hysteretic behaviors, onset temperatures of the dc magnetization for warming and cooling runs were measured and averaged. Values of T_C for the $y=0.13, 0.4$, and 0.5 samples were found to be 238 ± 2 , 155 ± 3 , and 120 ± 3 K, respectively.

Near normal incidence reflectivity spectra, $R(\omega)$, were measured between 0.01 and 30 eV. A liquid He-cooled

cryostat was used to measure T -dependence of $R(\omega)$ in a frequency region between 0.01 and 2.5 eV. Optical conductivity spectra, $\sigma(\omega)$, were obtained using the Kramers-Kronig transformation with appropriate extrapolations [10].

Figure 1 shows $\sigma(\omega)$ of the LPCMO samples below 2.0 eV. Note that $\sigma(\omega)$ of all the samples are very similar at 290 K: each of $\sigma(\omega)$ has a broad absorption feature centered around 1 eV and vanishes as ω approaches to zero. These gap-like features are consistent with the fact that these samples are in insulating states at room temperature. For $\text{Pr}_{0.7}\text{Ca}_{0.3}\text{MnO}_3$, $\sigma(\omega)$ are nearly T -independent, since it remains in an insulating state down to 15 K. For the samples with $y=0.13$, 0.4 and 0.5, $\sigma(\omega)$ show quite strong T -dependence. As T decreases below T_C , the spectral features approximately above 0.5 eV decrease and those below 0.5 eV increase. Interestingly, for the $y=0.4$ sample, such SW changes at all temperatures occur around one balancing point, fixed near 0.5 eV [14].

Note that some of $\sigma(\omega)$ show a double peak structure. For example, the $y=0.4$ sample displays two peaks centered around 0.25 and 1.5 eV at 120 K. The double peak feature is quite similar to that of two mid-gap states observed in the doping dependent $\sigma(\omega)$ of $\text{La}_{1-x}\text{Ca}_x\text{MnO}_3$ [15]. Based on this similarity, we attribute the absorption band near 1.5 eV to an intra-atomic transition between JT split e_g states [15,16], and the mid-IR absorption peak below 0.5 eV to an interatomic charge transfer transition between $\text{Mn}^{3+}(e_g^1)$ and $\text{Mn}^{4+}(e_g)$ with the same t_{2g} background spins [7,8,15]. In our recent paper on LCMO, we proposed that the mid-IR band below 0.5 eV come from incoherent absorption of a large polaron [10].

In Fig. 1, as y increases, the mid-IR absorption features decrease systematically. To get further understanding on the mid-IR absorption band, an effective carrier number, $N_{eff}(\omega_c)$, of carriers below a cut off frequency, ω_c , was evaluated using the following relation:

$$N_{eff}(\omega_c) = \frac{2m}{\pi e^2 N} \int_0^{\omega_c} \sigma(\omega) d\omega, \quad (1)$$

where m is an electron mass of carriers and N is a number of Mn ions per unit volume. For actual evaluation, the value of $\hbar\omega_c$ was chosen as 0.5 eV [17]. And, in evaluating N , T -dependent volume change was considered properly from reported structural data [18].

Figure 2 shows $N_{eff}(\omega_c)$ vs T curves for $y=0.13$ (solid circles), 0.4 (solid squares), and 0.5 (crosses). For comparison, values of $N_{eff}(\omega_c)$ for the LCMO sample (open diamonds) are also included [10]. It is found that the $N_{eff}(\omega_c)$ vs T curve for LCMO is quite close to that of the $y=0.13$ sample. [The T_C value of LCMO is 245 ± 2 K, which is close to that of the $y=0.13$ sample.] Note that $N_{eff}(\omega_c)$ for each sample increases abruptly near T_C . As the Pr doping increases, $N_{eff}(\omega_c)$ decreases systematically at overall temperatures.

In Fig. 2, it is interesting to note that the shape of $N_{eff}(\omega_c)$ for each sample is quite similar. And, the increasing rate of $N_{eff}(\omega_c)$ is nearly as same as that of T_C : for example, when T_C is reduced by about a factor of 2, $N_{eff}(\omega_c)$ is also reduced by a similar factor. So, we plotted $N_{eff}(\omega_c)/T_C$ vs T/T_C curves, shown in Fig. 3. Interestingly enough, even if detailed SW transfer behaviors in Fig. 1 are quite different, all of experimental values of $N_{eff}(\omega_c)/T_C$ fall into nearly in one curve. The result demonstrates that the $N_{eff}(\omega_c)/T_C$ vs T/T_C curves in these LPCMO compounds can be described by one scaling function. Moreover, the scaling function is very close to $\gamma_{DE}(T)$, which is the T -dependent DE bandwidth predicted by Kubo and Ohata [19]. The solid line in Fig. 3 displays the behavior of $\gamma_{DE}(T/T_C)$.

To explain this scaling behavior in the $N_{eff}(\omega_c)/T_C$ vs T/T_C curves, we adopt theoretical results by Röder *et al.* [11], who investigated a Hamiltonian including the DE interaction and the JT electron-phonon coupling terms. [A similar Hamiltonian was also investigated by Millis *et al.* [6,7].] After the Lang-Firsov transformation for the electron-phonon problem, the Hamiltonian could be reduced to an effective Hamiltonian over a phonon vacuum:

$$\tilde{H} = -t\xi(\eta) \sum_{\langle ij \rangle \sigma} \cos \frac{\theta_{ij}}{2} \left(c_{i\sigma}^\dagger c_{j\sigma} + H.c. \right) + \sum_i D_i, \quad (2)$$

where t is the bare hopping matrix element. The polaronic band narrowing is given by $\xi(\eta) = \exp(-\epsilon_p \eta^2 / \hbar \omega_0)$ with an effective electron-phonon coupling parameter ϵ_p and a coupled phonon frequency ω_0 . Here, η measures the degree of the polaron effect, which is determined self-consistently and dependent on ϵ_p , ω_0 , and the hole carrier concentration, x . Note that $\xi(\eta)$ is quite sensitive to a variation of t since ϵ_p is inversely proportional to t . D_i refers to diagonalized terms over the phonon vacuum. [For zero electron-phonon coupling, $\xi(\eta)$ simply becomes 1.] Within the Hamiltonian given in Eq. (2), Röder *et al.* [11] derived

$$T_C(x) = \frac{9}{50} [-e_B(x)] \xi(\eta), \quad (3)$$

where $e_B(x)$ is a band energy, which is proportional to t and depends on x . As η approaches zero, $e_B(x)$ is roughly proportional to $x(1-x)$.

If we assume that the mid-IR absorption below 0.5 eV should be proportional to the hopping term in Eq. (2),

$$N_{eff}(\omega_c; T) \approx t\xi(\eta) \langle \cos(\theta/2) \rangle \approx t\xi(\eta) \gamma_{DE}(T). \quad (4)$$

In the latter approximation, the spin-dependent cosine term was averaged thermodynamically and replaced with the mean field result, i.e. $\gamma_{DE}(T)$. Note that, in Eqs. (3) and (4), both $N_{eff}(\omega_c; T)$ and T_C include the same factor $\xi(\eta)$, which represents the polaronic band narrowing effect [20,21]. For all the LPCMO samples, the hole concentration can be considered to be fixed, i.e. 0.3 per

Mn atom, so $N_{eff}(\omega_c; T)/T_C$ should be proportional to $\gamma_{DE}(T)$. Indeed, the inset of Fig. 3 shows such a linear relationship.

As far as we know, the theory by Röder *et al.* [11] is the only model that can explain the scaling behavior. In this model, both T_C and the interatomic transfer matrix between $Mn^{3+}(e_g^1)$ and $Mn^{4+}(e_g)$ will be significantly affected at the same time by changes in the polaronic band narrowing factor. The variation of t was estimated to be less than 2 % in the LPCMO compounds under the tight-binding approximation [18]. Note that the small change in t is difficult to explain the large variations in $N_{eff}(\omega_c; T)$ and T_C without the self-amplifying coupling of both DE and JT effects [11]. Moreover, Röder *et al.* [11] predicted that a large polaron state should exist at a low temperature and that such an electron-phonon interaction should be also coupled with the spin degree of freedom. If such a large polaron state exists, as we demonstrated in our earlier paper [10], it should be in a strong electron-phonon coupling limit, which has not been realized in other real system before.

In Fig. 3, there are small discrepancies between experimental data and $\gamma_{DE}(T)$. For the samples of $y=0.4$ and 0.5, the experimental data are slightly deviated from $\gamma_{DE}(T)$ near T_C : the increase of $N_{eff}(\omega_c)$ near T_C is rather gradual. [This behavior might be related to the dc resistivity behavior, showing a broader M-I transition for a sample with a larger Pr doping [12].] Note that the $y=0.7$ sample, i.e. $Pr_{0.7}Ca_{0.3}MnO_3$, is a canted antiferromagnetic insulator [22]. Therefore, the observed discrepancies might be related to enhanced spin fluctuations near T_C due to the increased antiferromagnetic spin interaction relative to the ferromagnetic one.

As shown in Fig. 1, below T_C , a broad SW between 0.5 and 1.5 eV starts to decrease and a Drude peak and a broad mid-IR peak below 0.5 eV starts to appear. In the large polaron picture, these SW changes can be interpreted such that there is a collapse of the JT small polaron and a gradual crossover to the large polaron state as the sample enters the ferromagnetic metallic state. However, quite an unusual behavior was observed in the far-IR spectra.

Figure 4 shows the far-IR $\sigma(\omega)$ of LPCMO. Estimated dc conductivity values from the Hagen-Rubens relation [13], which were denoted as symbols, agree reasonably well with the extrapolated values of $\sigma(\omega)$ as $\omega \rightarrow 0$. For a metallic sample, as ω decreases, $\sigma(\omega)$ increases initially but shows a downturn at a very low frequency. Such a trend becomes more evident, as y increases, i.e. as the carrier hopping parameter is reduced. [For a pure LCMO sample, we could not observe such an effect up to a measured frequency limit of 8 meV [10].] Therefore, the Drude peak seems to disappear systematically with increasing the Pr doping, even if the sample shows a metallic transport behavior below T_C . This observation suggests that the LPCMO samples with large Pr

doping, i.e. $y=0.4$ and 0.5, are far from normal Fermi liquids at low T . Similar behaviors of $\sigma(\omega)$ in the far-IR region were also observed in a layered manganites [23] and $La_{1-y}TiO_{3-\delta}$ [24].

We postulate that the unusual far-IR response of $\sigma(\omega)$ be caused by the Anderson localization effects. Many theoretical works predicted that disorder effects could be important in the CMR manganites [25]. For the LPCMO samples, there are several possible causes which bring out randomness in the effective hopping matrix: (1) Mn-O-Mn bond angle and/or length disorder, (2) inhomogeneous JT lattice distortions, (3) spin-exchange interaction between the Pr and the Mn ions, and (4) competition between the ferromagnetic DE and the antiferromagnetic superexchange interaction among the Mn sites [26]. Such randomness sources can produce a mobility edge which is located close to the Fermi energy, resulting in the suppression of the Drude peak. And, for a sample with a smaller value of the carrier hopping term, i.e. a higher Pr doping, its carrier transport will be affected more easily by the mobility edge, so the Anderson localization effects should be more significant in its far-IR conductivity spectrum.

In summary, we investigated the SW changes, especially in the mid-IR region, of the $La_{0.7-y}Pr_yCa_{0.3}MnO_3$ samples. The Pr doping results in suppression of the far-IR conductivity, probably due to the Anderson localization. It was also found that the experimental data of $N_{eff}(\omega_c)/T_C$ could be scaled into a curve, which is linearly proportional to $\gamma_{DE}(T)$, regardless of the Pr doping value. This interesting scaling behavior was explained in terms of the theoretical model by Röder *et al.*, which takes into account of a JT coupling in the DE model. This work clearly shows the importance of the lattice effects in the optical properties of the CMR manganites.

One of us (TWN) appreciate the hospitality of the LG-CIT during his visit when this manuscript was written. We acknowledge the financial support by Ministry of Education through the grant No. BSRI-97-2416 and by the Korea Science and Engineering Foundation through the grant No. 96-0702-02-01 and through RCDAMP of Pusan National University. Reflectivity measurements in the vacuum ultraviolet region were performed at Pohang Light Source, supported by POSCO and Ministry of Science and Technology.

*Also at LG Corporate Institute of Technology (LG-CIT), Seoul, Korea. Electronic mail address: twnoh@phya.snu.ac.kr.

[1] C. Zener, Phys. Rev. **82**, 403 (1951); P. W. Anderson and H. Hasegawa, *ibid.* **100**, 675 (1955); P. G. de Gennes, *ibid.*

118, 141 (1960).

- [2] Y. Okimoto *et al.*, Phys. Rev. Lett. **77**, 109 (1995).
- [3] Y. Okimoto *et al.*, Phys. Rev. B **55**, 4206 (1997).
- [4] S. Ishihara, M. Yamanaka, and N. Nagaosa, Phys. Rev. B **56**, 686 (1997).
- [5] P. E. de Brito and H. Shiba, Phys. Rev. B **57**, 1539 (1998).
- [6] A. J. Millis, B. I. Shraiman, and R. Mueller, Phys. Rev. Lett. **77**, 175 (1996).
- [7] A. J. Millis, R. Mueller, and B. I. Shraiman, Phys. Rev. B **54**, 5389 (1996); *ibid.*, 5405 (1996).
- [8] S. G. Kaplan *et al.*, Phys. Rev. Lett. **77**, 2081 (1996).
- [9] K. H. Kim *et al.*, Phys. Rev. Lett. **77**, 1877 (1996).
- [10] K. H. Kim, J. H. Jung, and T. W. Noh, Report No. cond-matt/9804167.
- [11] H. Röder, J. Zhang, and A. R. Bishop, Phys. Rev. Lett. **76**, 4987 (1996).
- [12] H. Y. Hwang *et al.*, Phys. Rev. Lett. **77**, 1877 (1995).
- [13] K. H. Kim *et al.*, Phys. Rev. B **55**, 4023 (1997).
- [14] A similar spectral weight change at a fixed balancing frequency, called the ‘isosbetic point’, was observed for (Sm,Ca)TiO₃. Refer to T. Katsufuji, Y. Okimoto, and Y. Tokura, Phys. Rev. Lett. **75**, 3497 (1995). However, in this case, the spectral changes occurred by varying the hole doping concentration, not the temperature.
- [15] J. H. Jung *et al.*, Phys. Rev. B (to be published in 1 May 1998).
- [16] J. H. Jung *et al.*, Phys. Rev. B **55**, 15 489 (1997).
- [17] Even if ω_c is chosen with a slightly different value, e.g. 0.6 eV, the shape of the SW changes and their scaling behaviors are nearly the same with those shown in Figs. 2 and 3.
- [18] P. G. Radaelli *et al.*, Phys. Rev. B **56**, 8265 (1997).
- [19] K. Kubo and N. Ohata, J. Phys. Soc. Jpn. **33**, 21 (1972).
- [20] G. D. Mahan, *Many-Particle Physics* (Plenum, New York, 1990), Chaps. 4 and 6.
- [21] J. D. Lee and B. I. Min, Phys. Rev. B **55**, 12 454 (1997).
- [22] H. Yoshizawa *et al.*, Phys. Rev. B **52**, R13 145 (1995).
- [23] T. Ishikawa *et al.*, Phys. Rev. B **57**, R8079 (1998).
- [24] D. A. Crandles *et al.*, Phys. Rev. B **49**, 16 207 (1994).
- [25] L. Sheng *et al.*, Phys. Rev. B **56**, R7054 (1997); Qiming Li *et al.*, Phys. Rev. B **56**, 4541 (1997).
- [26] J. M. D. Coey *et al.*, Phys. Rev. Lett. **75**, 3910 (1995).

FIG. 1. Optical conductivity spectra of La_{0.7-y}Pr_yCa_{0.3}MnO₃ below 2.0 eV.

FIG. 2. T -dependence of N_{eff} ($\omega_c = 0.5$ eV) for La_{0.7-y}Pr_yCa_{0.3}MnO₃.

FIG. 3. $N_{eff} (\omega_c = 0.5$ eV)/ T_C vs T/T_C curves of La_{0.7-y}Pr_yCa_{0.3}MnO₃. The solid line refers to the behavior of $\gamma_{DE}(T) \equiv \langle \cos(\theta/2) \rangle$. The inset shows a linear scaling behavior between $N_{eff} (\omega_c = 0.5$ eV)/ T_C and $\gamma_{DE}(T)$.

FIG. 4. Optical conductivity spectra of La_{0.7-y}Pr_yCa_{0.3}MnO₃ in the far-infrared region below 0.15 eV. Symbols denote the dc conductivity values estimated from the Hagen-Rubens relation.

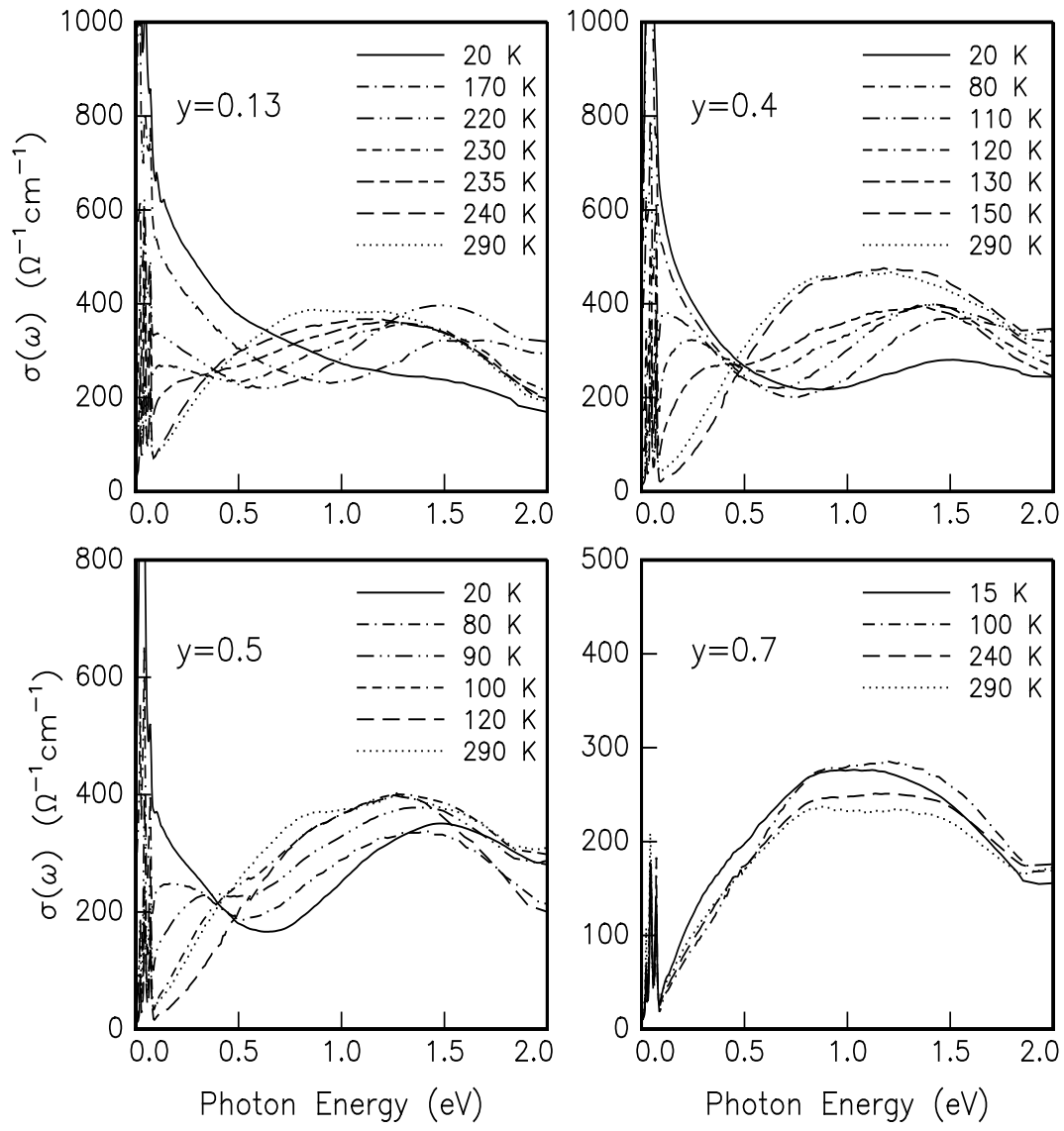


FIG. 1. K. H. Kim *et al.*

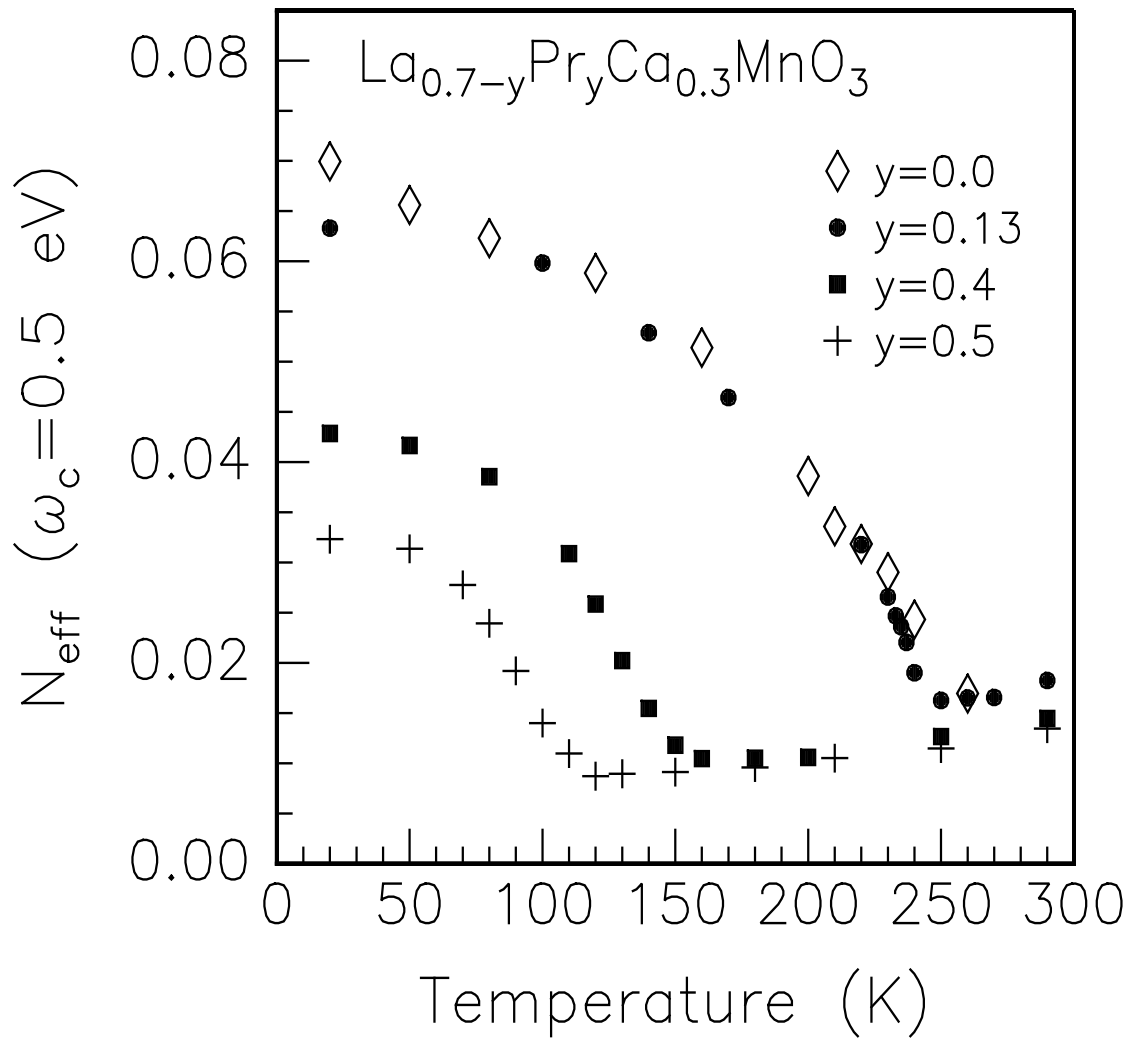


FIG. 2. K. H. Kim *et al.*

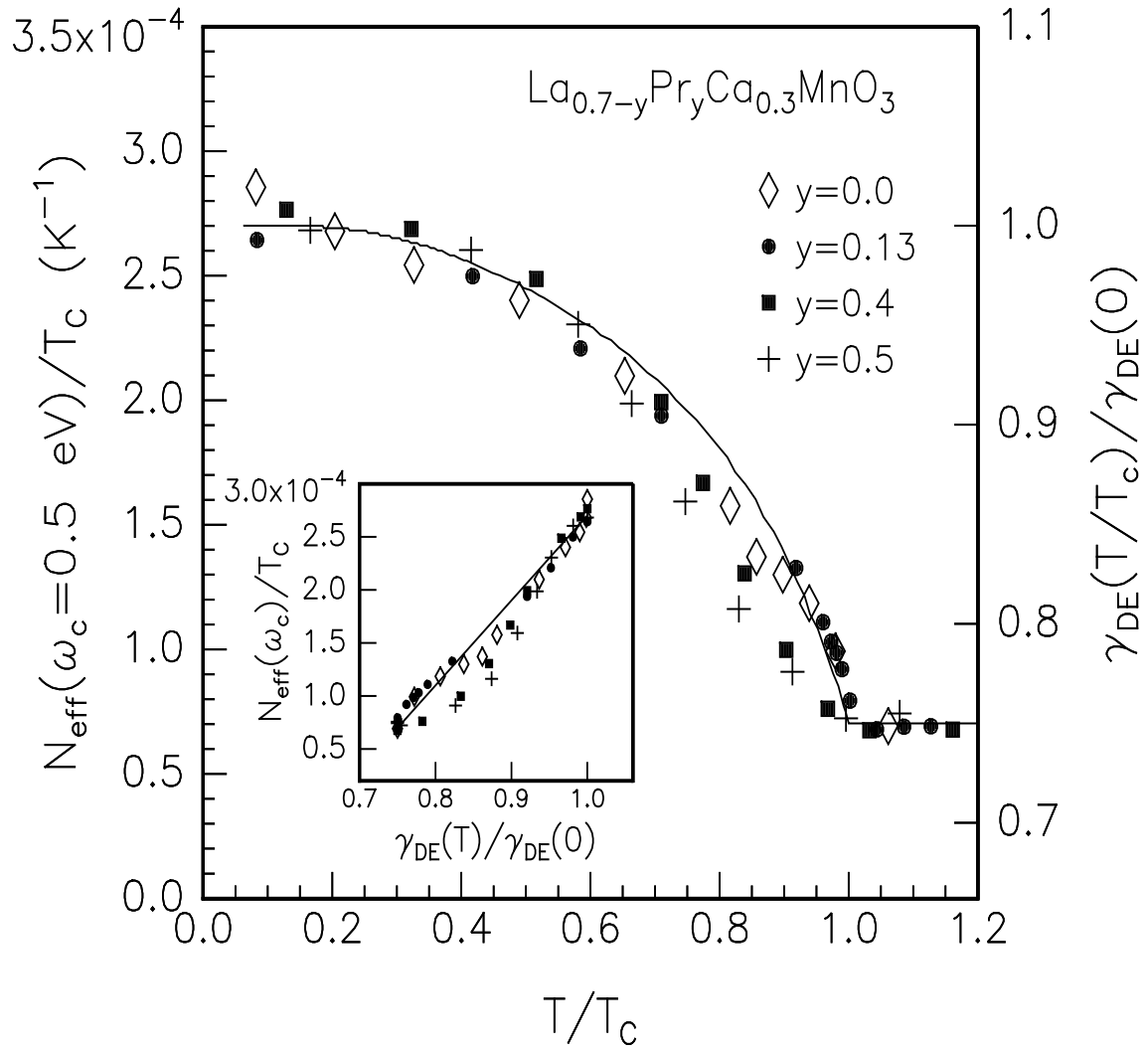


FIG. 3. K. H. Kim *et al.*

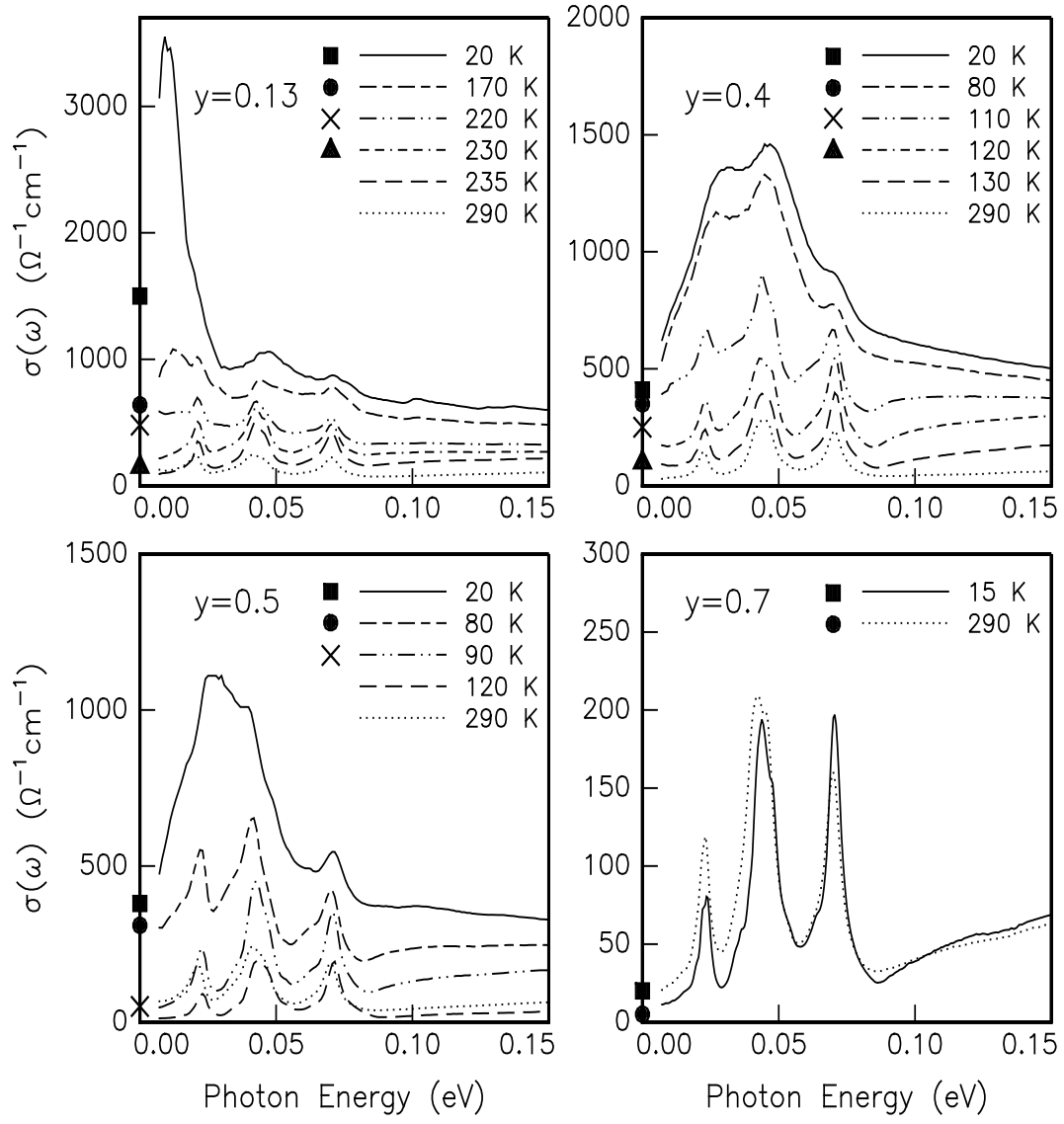


FIG. 4. K. H. Kim *et al.*